18

Photocontrolled reversible changes in the electronic and vibrational spectra of photochromic diarylethene in various nanostructured systems

© G.T. Vasilyuk[1], P.V. Karpach[1], S.D. Gogoleva[1], A.O. Ayt[2], V.A. Barachevsky[2], S.A. Maskevich[3]

[1] Yanka Kupala Grodno State University,
230023 Grodno, Belarus
[2] Photochemistry Center, Russian Academy of Sciences,
119421 Moscow, Russia
[3] Belorussian State University, International Sakharov Environmental Institute BSU,
220070 Minsk, Belarus

e-mail: vasilyuk@grsu.by

Received December 10, 2021
Revised December 20, 2021
Accepted December 22, 2021

An analysis of the results of complex experimental and theoretical studies of photoinduced changes in the spectral properties of photochromic diarylethene in various nanostructured systems is presented. The properties of diarylethene were studied in solutions in the presence of colloidal metal and semiconductor nanoparticles, as well as in the form of solid-phase composite nanostructured core-shell systems based on colloidal nanoparticles with a shell of diarylethene molecules (including in a polymer matrix). A photoinduced reversible change in the electronic and vibrational spectra of diarylethene in various studied matrices was found. The results can be used to create optoelectronic photo-switchable elements for ultra-high-capacity memory devices, photo-controlled molecular switches and sensors.

Keywords: photochromism, diarylethenes, nanocomposites, quantum dots, electronic spectra, vibrational spectra, fluorescence, Ferster resonance energy transfer, quantum chemical calculations.

DOI: 10.21883/EOS.2022.03.53563.3023-21

Introduction

One of development areas in the modern electronics is design of hybrid devices, whose properties depend on the molecular structure of the used compounds, with the potential of use in optical integrated circuits [1,2]. For these purposes, photochromic compounds are most promising, especially thermally irreversible diaryl ethenes (DAE) [3–5], irreversibly changing their properties when exposed to light and used to design photoswitches of various types [6].

Nanostructured photochromic hybrid (composite) systems [7], including molecules of photochromic organic compounds, in particular, from DAE class, and nanoparticles of noble metals, namely gold [8–14] and silver [9,15,6], as well as inorganic semiconductors [17] are of special interest.

Previously the possibility was theoretically predicted [18,19] and experimentally studied [20,21] to improve efficiency of photochemical processes together with amplification of the signal of Raman scattering (RS) of light and luminescence when molecules are adsorbed on the metal surface with nanosized irregularities related to plasmon effects (fig. $1, a$). Properties of photochromic compounds next to nanostructured surface of noble metals were also studied experimentally [22].

Plasmon amplification of electromagnet field near a metal nanoparticle provides for higher effectiveness of photochromic transformations both because of formation of two-photon photochromic reaction of DAE cycloreversion, and 2-5-fold increase of one-photon reaction speed [23]. Isomerization of a switch (photochromic molecule) causes variation of its electronic properties, thus varying dielectric permeability in close proximity to the nanoparticle surface, which makes it possible to reversibly control plasmon resonance frequency and interparticle interaction [23].

In promising molecular systems, containing fluophor (for example, a semiconductor quantum point (QD CdSe/ZnS) and a photochromic fragment, phototransformation of a photochromic molecule may cause modulation of fluorescence intensity through variation of quantum yield of fluorophor (with inductive-resonant energy transfer (FRET) from fluorophor to photochrome), and also as a result of reabsorption of fluorescence light by photochromic compound (effect of internal filter) [23–25].

Based on composite structures „nanoparticle–molecular switch " it is possible to create nanosystems operating in non-equilibrium mode, which may change the internal procedure (structure) and adapt to external effects.

This paper (to develop previous research of authors [26–34]) presents analysis of results from comprehensive experimental and theoretical study of photoinduced changes of spectrial properties of photochromic DAE1 in various environments. According to the results of previous studies, DAE1 has free photochromic properties (light sensitivity and amplitude of dynamic variation of spectral photoabsorption)

both in solutions and in solid-phase films. The study of this compound properties is of utmost interest in nanocomposite structures (systems) with metal nanoparticles — for potential use in photocontrolled switches of electric and optic signal [4,23] or sensors [23], and also with semiconductor nanoparticles — for use in fluororescent photoswitched chemosensors and multifunctional photo- and electrically controlled displays [23].

Experimental part

The objects of research in this paper were a photochromic compound DAE1 from class of cyclopentene derivatives of DAE, and also composite systems based on molecules of this compound, containing nanoparticles of silver, gold or CdSe/ZnS (including films and polymer nanospheres, which contain semiconductor QDs CdSe/ZnS and DAE1 molecules, scheme 1).

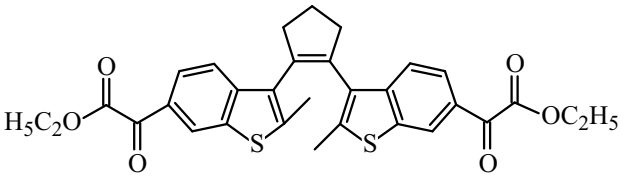

DAE1

The spectral characteristics and structure of photochromic nanocomposites obtained in solutions and solid-phase films and their changes during photochromic transformations were studied using spectrophotometry, vibrational spectroscopy (infrared (IR) absorption, Raman Scattering (RS) and Surface Enhanced Raman Scattering (SERS) of light and quantum chemistry methods. The photoinduced modulation of the fluorescence in such systems, including that due to FRET, was studied by steady-state and kinetic fluorimetry methods.

Silver nanoparticles with sizes of 30–40 nm were obtained by citrate reduction of silver ions in aqueous solution [35], and those with sizes of 8–10 nm — borohydride reduction of silver in aqueous solution [36]. Gold nanoparticles with a diameter of about 20 nm were prepared by citrate reduction of gold in aqueous solution [37,38]. To prepare silver and gold colloidal films, a method of layer-by-layer deposition of silver colloids (or nanocomposite systems of noble metal particles with a shell of photochromic DAE molecules) was used by dipping a glass substrate into a colloidal solution and subsequent drying [26]. The maximum of plasmonic absorption band of solid-phase systems based on silver borohydride sol is located at 415 nm and that based on citrate sol — about 428 nm. To obtain nanocomposite systems containing silver or gold nanoparticles with a shell of photochromic DAE molecules (fig. 1, *a*), solutions of noble metal nanoparticles and photochromic compounds were mixed at a volume ratio of 1 : 1 [26].

The semiconductor nanoparticles — CdSe/ZnS QDs containing a CdSe core and a passivating shell of the wider-band-gap ZnS material used in this paper were synthesized at the Research Institute for Physical Chemical Problems of the Belarusian State University according to an adapted protocol.

The photochromic systems based on DAE and QD CdSe/ZnS were prepared in chloroform or toluene using methods [30]. In addition, polymeric nanospheres synthesized according to the method of Professor M.V. Artemyev [31] were used, which included semiconducting QDs and molecules of photochromic DAE1 compound (fig. 1, *b*). To obtain such polymeric nanospheres, the method of introducing DAE1 molecules into a thin polymer shell on top of hydrophobic CdSe/ZnS QDs during their encapsulation and solubilization in water using the well-known procedure [39] was applied.

Spectral and kinetic studies of photochromic transformations of DAE in solutions and in composite nanostructures were performed using SPECORD 200 (Carl Zeiss, Germany) and Cary 50 Bio (Varian, Australia) spectrophotometers, as well as LC-4 lamp (Hamamatsu, Japan). A UV filter UFS-1 was used to isolate the UV component of the radiation. Irradiation of samples with visible light was carried out through light filter ZhS-16. In some cases LEDs with maximum bands at 365 (LED365) and 514 nm (LED514) were used for irradiation. Half-widths of the LED365 and LED514 light diodes radiation were 9 and 32 nm, and the optical power — 0.45 and 3 W, respectively. The irradiation time required to translate the DAE between forms A and B was determined from the absorption spectra measured in the equilibrium state. Possible scattering and reflection from the sample were not taken into account when recording the absorption spectra.

IR spectra were recorded using Nicolet iS10 FTIR spectrometer (Thermo Scientific, USA). 3D scanning confocal Raman microscope with Nanofinder S spectrometer (Solar TII, Belarus) was used for registration of RS and SERS spectra. RS and SERS spectra of the studied objects were recorded in the range of 200–1800 cm^{-1}. The power density of laser radiation on the sample was 5–10 mW/mm^2.

Spectrofluorimeter SM2203 (Solar, Belarus) was used to record the fluorescence spectra, and the laboratory setup described in [40], operating in time-correlated photon counting mode (TCSPC) [41], was used to measure the fluorescence decay time. The excitation source was a PDL 800B picosecond diode laser with LDH-405 and LDH-470 laser heads (PicoQuant, Germany), which generates light pulses of 70 ps duration with a repetition rate up to 40 MHz and wavelengths of 407 and 467 nm respectively. The registration system includes a PMA-182 photoelectric detector and a TimeHarp200 time-correlated photon counting system from PicoQuant (Germany).

Results of quantum-chemical calculations were used to interpret vibration and electron spectra. In this paper all quantum chemical calculations are made using software

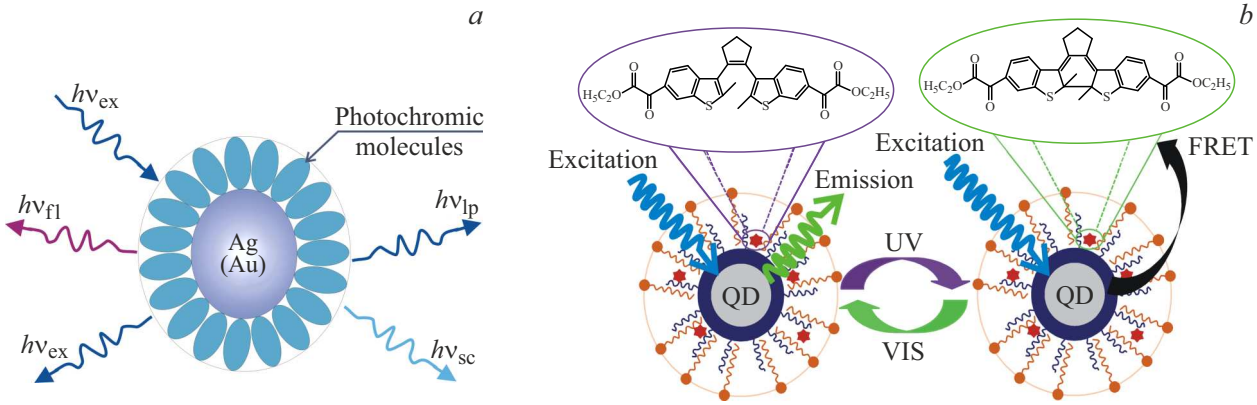

Figure 1. (*a*) Schemes of optical processes in solid-phase photochromic nanocomposite systems based on metal nanoparticles and (*b*) photoinduced modulation of fluorescence of nanocomposite polymer nanospheres containing a semiconductor nanoparticle (QD) and molecules of DAE1 in process of photochromic transformations of DAE.

suite PC GAMESS 7.1.G (Firefly). Equilibrium geometry and vibration spectra of DAE1 molecule are calculated using RHF method. Vibration (IR and RS) spectra of molecules were calculated using basis 6-31G. Calculation of potential energy surface (PES, surface cross section) depending on the distance between atoms of carbon participating in photoisomerization reaction, was made using density functionality theory (DFT) methods, hybrid three-parameter exchange Becke functionality with correlation functionality Lee–Yang–Parr (B3LYP) [42–44]. To calculate energy of main (S_0) and excited (S_1, S_2, S_3) states, DFT and TDDFT methods were used accordingly (using B3LYP functionality and 6-31G basis). PES cross section of DAE1 molecule was obtained with using the reaction coordinate in the form of distance between carbon atoms, where linkage is formed (broken) in process of reversible photoisomerization reaction. PES cross section of the main state was obtained by DFT method through fixation of the mentioned distance (at every value of such distance — reaction coordinate) and optimization of the remaining structure of the molecule. When calculating PES cross sections of states S_1, S_2, S_3, TD DFT method was used, as well as molecule geometry in every point produced during calculation of PES of the main state S_0.

Results and discussion

Calculation of DAE1 electron structure and its phototransformations

Photochromic transformations of DAE are caused by reversible valent photoisomerization between open (A) and cyclic (B) forms (scheme 2) [3–5]:

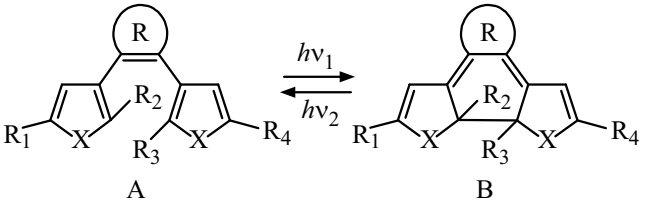

Open colorless isomer A, absorbing UV radiation, is reversibly transformed into colored isomer B, which, when exposed to visible radiation absorbed by it, turns again into the initial open isomer. A distinctive feature of photochromic DAE is thermodynamic resistance of both isomers.

To interpret results produced by experimental methods of electron spectroscopy, and also to analyze mechanisms of photoinduced transformations of DAE1 molecule, quantum chemical study of electron structure and properties of this molecule was conducted. Results (estimated spectra of electron absorption and cross section of PES states S_0, S_1, S_2, S_3 of DAE1 molecule) are given in fig. 2, 3 and in table 1, 2.

From fig. 2, *a* and table 1 it is seen that for open isomer DAE1 the most intense absorption bands (with maximum at 333 nm and oscillator power 0.39; with maximum at 402 nm and oscillator power 0.15) are related to transitions in excited singlet states of molecule: $S_0 \rightarrow S_7$, $S_0 \rightarrow S_3$ accordingly. Excitation of electron with 145 molecular orbital (MO) to 148 MO makes the main contribution to absorption band at 333 nm; from 147 MO (HOMO) to 148 MO (LUMO) — to absorption band at 402 nm (fig. 2, *b*). Calculation results demonstrate that when DAE1 molecule is radiated in a long-wave absorption band of open form A, transition $S_0 \rightarrow S_3$ takes place, related to transition of charge from alken fragment and thiophen rings (including from sulfur atoms) to end groups of DAE1 molecule. Besides, transition $S_0 \rightarrow S_1$ has near-zero probability.

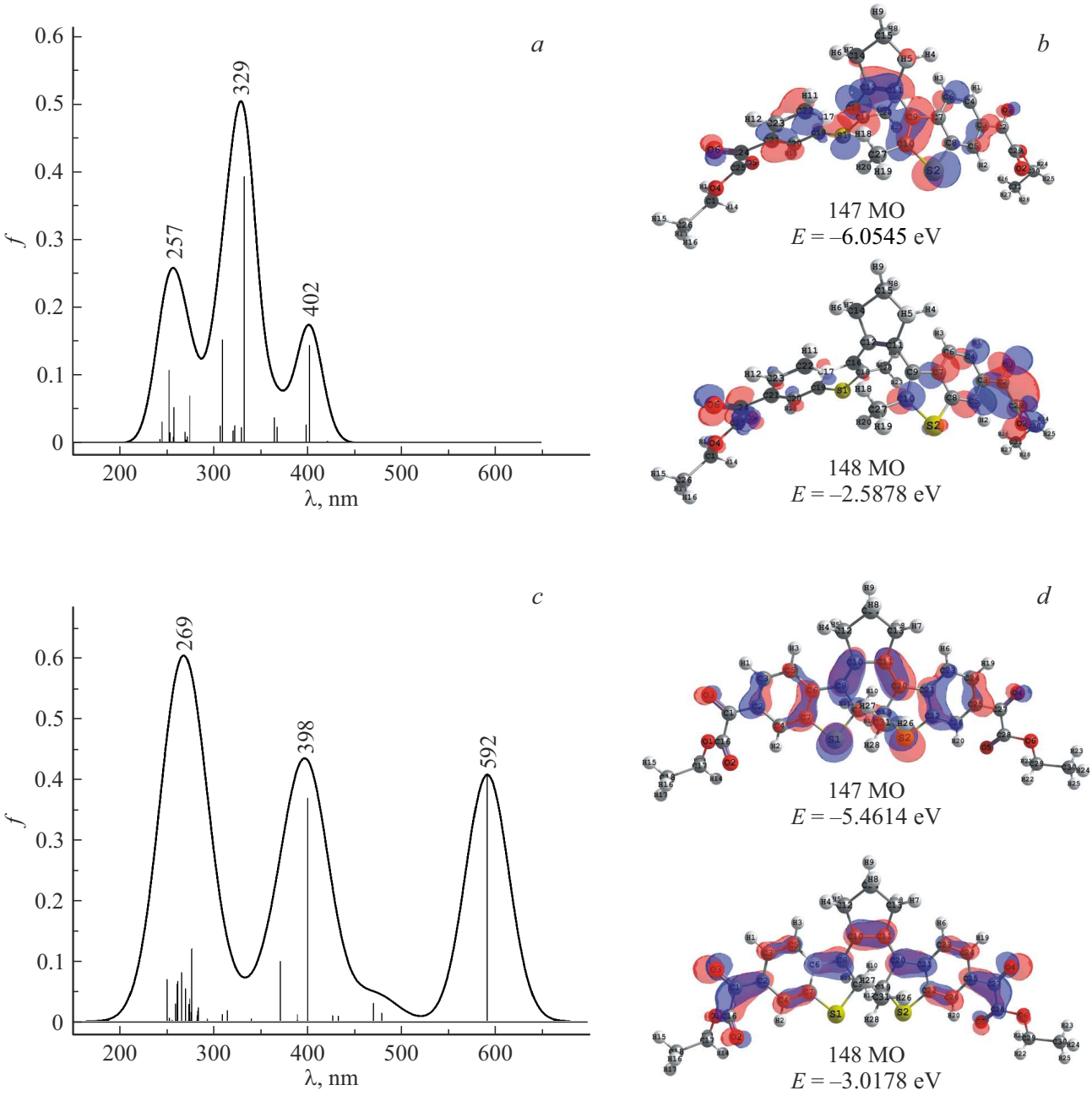

Figure 2. Calculated spectra of electronic absorption (a, c), shapes of boundary MOs involved in formation of DAE1 absorption spectrum (b, d) of open (a, b) and cyclic (c, d) isomers of DAE1 molecule.

For closed (cyclic) isomer DAE1 (fig. 2, *c* and table 1) the most intense absorption bands (with maximum at 401 nm and oscillator power 0.37; with maximum at 592 nm and oscillator power 0.41) are related to transitions in excited singlet states of molecule: $S_0 \rightarrow S_6$, $S_0 \rightarrow S_1$ accordingly. Excitation of electron with 145 MO to 148 MO makes the main contribution to absorption band at 401 nm; from 147 MO (HOMO) to 148 MO (LUMO) — to absorption band at 592 nm (fig. 2, *d*). As a result of DAE1 molecule radiation in long-wave absorption band of cyclic form B, $\pi - \pi^*$-transition $S_0 \rightarrow S_1$ takes place, localized in alken fragment and in thiophen and coupled rings, related to redistribution of charge in these fragments (at the same time charge is transferred from sulfur atoms). Specified redistribution of the charge leads to considerable improvement in DAE1 molecule electric conductivity, which makes it possible to treat this compound as promising for use in photocontrolled switches of electric signal.

In process of analysis of boundary molecular orbitals in DAE1 compound, the following were calculated: ionization potential $IP = -E_{\mathrm{HOMO}}$, electron affinity $E_A = -E_{\mathrm{LUMO}}$, total hardness $\eta = (IP - E_A)/2$, elec-

Table 1. Electron structure of open and cyclic isomers of DAE1 molecule calculated relative to main peaks

Isomer	State	λ, nm	ΔE, eV	Decomposition of wave functions along singly excited configuration	f
Open	$S_0 \rightarrow S_{23}$	253	4.90	$-0.61\,(146 \rightarrow 151) + 0.49\,(147 \rightarrow 152) - 0.40$ $(140 \rightarrow 149) - 0.20(145 \rightarrow 150)$	0.11
	$S_0 \rightarrow S_7$	333	3.72	$-0.78(145 \rightarrow 148) - 0.34(144 \rightarrow 149)$ $+0.29(145 \rightarrow 149) + 0.29(146 \rightarrow 149)$	0.39
	$S_0 \rightarrow S_3$	402	3.08	$-0.98(147 \rightarrow 148) + 0.09(143 \rightarrow 148) - 0.09$ $(145 \rightarrow 148)$	0.15
Cyclic	$S_0 \rightarrow S_{18}$	277	4.47	$-0.36(135 \rightarrow 148) + 0.35(142 \rightarrow 149) - 0.34$ $(137 \rightarrow 148) - 0.32(147 \rightarrow 152)$	0.12
	$S_0 \rightarrow S_6$	401	3.09	$-0.85(145 \rightarrow 148) - 0.36(146 \rightarrow 149) - 0.25$ $(147 \rightarrow 150)$	0.37
	$S_0 \rightarrow S_1$	592	2.09	$-0.99(147 \rightarrow 148) - 0.14(145 \rightarrow 148)$	0.41

Note. λ — transition wave length, ΔE — transition energy, f — oscillator power.

Table 2. Estimated electron properties of open and cyclic isomers of DAE1 molecule

Isomer	E_{HOMO}, eV	E_{LUMO}, eV	IP, eV	E_A, eV	E_g, eV	μ, eV	η, eV	S, eV	χ, eV	ω,eV
Open	−6.06	−2.59	6.06	2.59	3.47	−4.32	1.73	0.58	4.32	5.39
Cyclic	−5.46	−3.02	5.46	3.02	2.44	−4.24	1.22	0.82	4.24	7.36

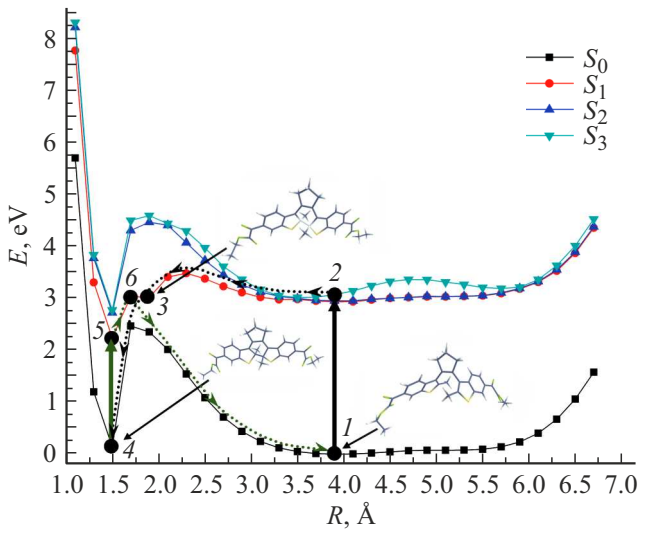

Figure 3. Cross sections of potential energy surfaces of states S_0, S_1, S_2 and S_3 of DAE1 molecule and routes of direct (points *1, 2, 3, 4*) and reverse (points *4, 5, 6, 1*) photochromic transformations.

tronegativity $\chi = (IP + E_A)/2$, electron chemical potential $\mu = -(IP + E_A)/2$, electrophilicity $\omega = \chi^2/2\eta$ and chemical softness $S = 1/\eta$.

Results of DAE1 compound boundary molecular orbitals analysis are given in table 2.

To analyze processes of photoinduced DAE1 molecule transformations, PES of states S_0, S_1, S_2, S_3 were calculated.

From fig. 3 you can see that in its main state the PES cross section of DAE1 molecule has two minima corresponding to open (colorless, around 3.9 Å) and closed (cyclic, colored, around 1.5 Å) forms. It should be noted that for an open isomer the minimum is rather wide, while for a cyclic isomer it is narrow. These isomers are divided by energy barrier with width of ~ 2.4 eV.

Before UV radiation DAE1 molecule is in open form (point 1, fig. 3), and after photoexcitation from state S_0 it changes (with transition energy 3.08 eV and oscillator power 0.15) to state S_3 (point 2). Then intra-conversion transition $S_3 \rightarrow S_1$, occurs, and for molecules to go to closed form (to achieve state 4 with minimum energy), it has to overcome energy barrier ~ 0.5 eV. Further return to PES of the main state S_0 takes place through transition over point 3 in cyclic form (point 4).

Under reverse photochromic transformation of DAE1 (from cyclic form to open one) after photoexcitation, DAE1 molecule from point 4 changes (with transition energy 2.09 eV and oscillator power 0.41) to excited state S_1 (point 5). For cycloreversion reaction to occur, the system should reach point 6 (around1.7 Å) and further change to point 1 (open isomer of DAE1 molecule).

Photoinduced changes of electronic spectra of photochromic nanostructured systems based on DAE1

All photochromic systems based on inorganic nanoparticles and DAE1 molecules that we studied undergo pho-

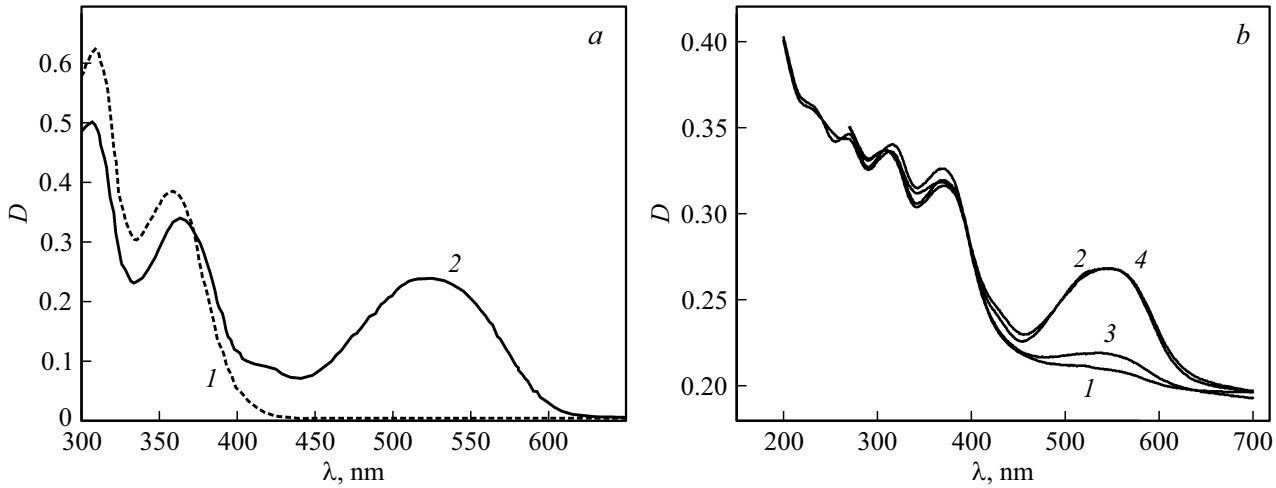

Figure 4. (*a*) DAE1 absorption spectra in solutions in DMSO before (curve *1*) and after (*2*) UV radiation with LC-4 lamp light through light filter UFS-1; DAE concentration in solution $C = 2 \cdot 10^4$ mol/dm^3, cuvette thickness 0.2 cm. (*b*) Absorption spectra of solid-phase composite nanostructured systems „metal nanoparticle-photochromic molecule" (*1, 2*) based on DAE1 and silver sols on quartz and solid-phase DAE1 films on quartz (without sols, *3, 4*) before radiation (*1, 3*) and after UV radiation through a light filter UFS-1 (*2, 4*) [26].

Table 3. Spectral characteristics of photochromic nanostructured systems based on DAE1 and metal nanoparticles (NP)

System	State	λ_A^{max}, nm (D_A)	λ_B^{max}, nm	ΔD_B^{phot}	$\Delta D_B^{phot}/D_A$
DAE1	Solution in DMSO	305 (0.61) 355 (0.40)	520	0.20	0.50
DAE1 + NP Ag		305 (0.62) 355 (0.40)	520	0.20	0.50
DAE1	Solution in mix ACN with water (1 : 1)	308 (0.82) 354 (040)	520	0.20	0.40
DAE1 + NP Au		308 (0.92) 354 (0.60)	520	0.20	0.33
DAE1	Solid-phase amorphous film	317 (0.13) 368 (0.12)	544	0.05	0.42
DAE1 + NP Ag		317 (0.13) 368 (0.12)	544	0.06	0.50
DAE1 + NP Au		310 (0.19) 364 (0.15)	544	0.07	0.47

Note. λ_A^{max} and λ_B^{max} — wave lengths of absorption band maxima of open A and cyclic B forms accordingly, D_A — maximum value of optical density in maximum of absorption band of open form A, ΔD_B^{phot} — maximum value of photoinduced optical density in maximum of long-wave absorption band of cyclic form B in photoequilibrium state, $\Delta D_B^{phot}/D_A$ — normalized optical density determining light sensitivity of compound.

toinduced reversible changes of absorption spectra. Results of comparative spectral-kinetic research of photochromic transformations of DAE1 (in a solution and solid phase) in absence and presence of silver and gold nanoparticles are given in table. 3 and in fig. 4. Absorption spectrum of DAE1 open form in dimethyl sulfoxide (DMSO) is characterized by two absorption bands with maxima at 305 and 355 nm (fig. 4, *a*, curve *1*, table 3). When exposed to UV light, a new absorption band appears in the visible region of the spectrum with maximum at 520 nm (fig. 4, *a*, curve *2*; table 3), caused by formation of cyclic form B. This compound manifests photochromic properties in solutions (in acetonitrile (ACN), methanol, toluene, DMSO) both in absence and in presence of silver and gold sols [26]. After introducing silver nanoparticles into the solution of the photochromic compound, the absorption bands of the open form A of DAE1 are not shifted. Llight sensitivity ($\Delta D_B^{phot}/D_A$) of DAE1 when noble metal nanoparticles are added to the solution either does not change (for Ag) or slightly decreases (for Au). Kinetic characteristics of phototransformations of DAE1 compound do no vary without and in the presence of metal nanoparticles.

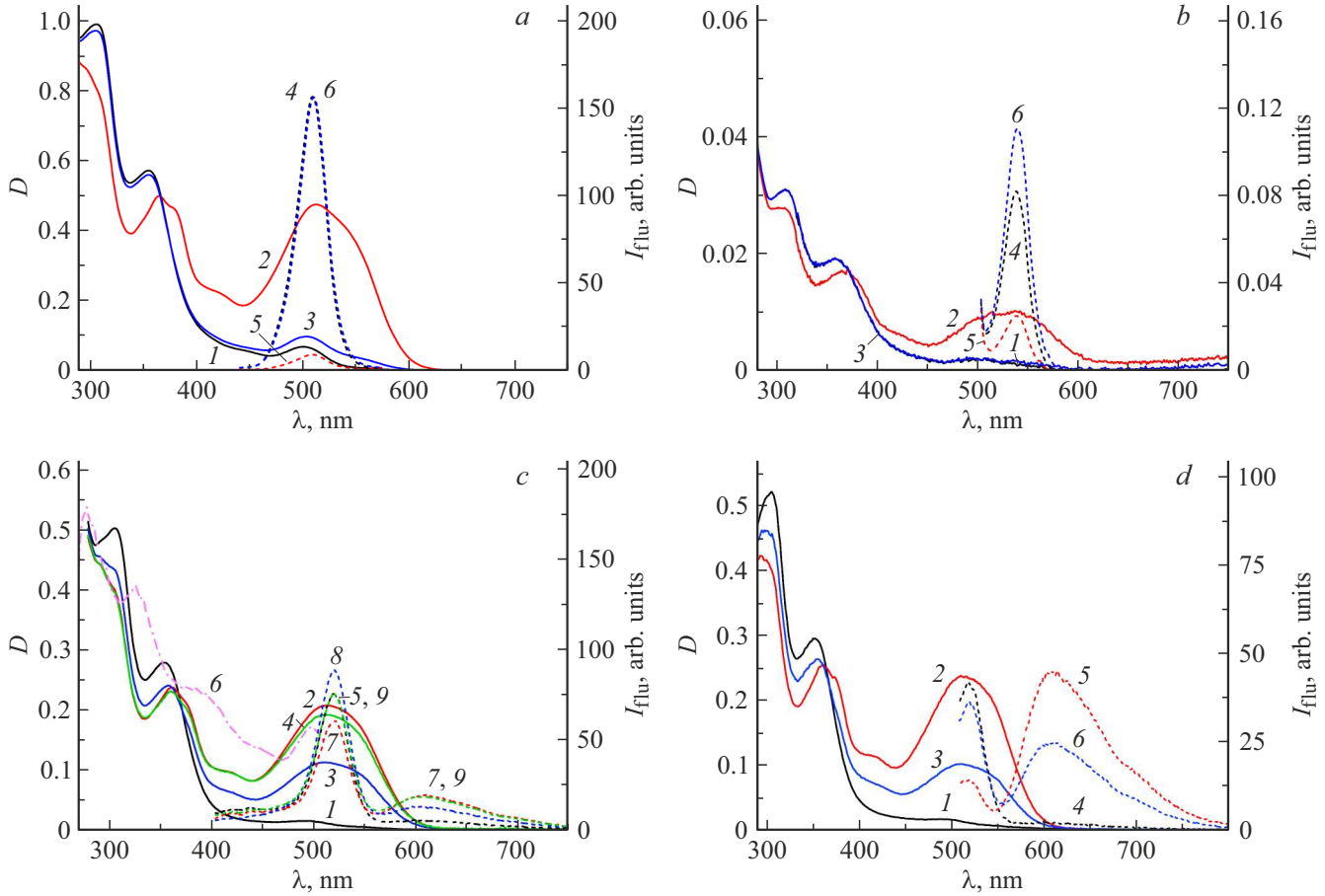

Figure 5. Spectra of absorption and fluorescence of photochromic system QD525-DAE1 in various matrices. (*a*) Spectra of absorption (curves *1*–*3*) and fluorescence on excitation wave length 440 nm (*4*–*6*) of system in toluene before (*1, 4*), after UV radiation (*2, 5*) and visible (*3, 6*) light exposure. (*b*) Spectra of absorption (*1*–*3*) and fluorescence on excitation wave length 440 nm (*4*–*6*) of solid-phase amorphous film of QD525-DAE1 before (*1, 4*), after UV radiation (*2, 5*) and visible (*3, 6*) light exposure. (*c*) Spectra of absorption (*1*–*4*), excitation of fluorescence when measured on wave length 516 nm (*6*) and fluorescence on excitation wave length 395 nm (*5, 7*–*9*) of system in polymer film PMMA before (*1, 5, 6*), after UV radiation (*2, 7*) and visible (*3, 8*) light exposure and after repeated UV radiation (*4, 9*). (*d*) Spectra of absorption (*1*–*3*) and fluorescence on excitation wave length 500 nm (*4*–*6*) of system in polymer film of copolymer AS before (*1, 4*), after UV radiation (*2, 5*) and visible (*3, 6*) light.

Absence of changes in the spectral-kinetic characteristics of DAE1 both in solutions and in solid-phase layers upon introduction of nanoparticles (table 3) can be explained by the fact that the molecules of this compound experience physical interaction with the surface of nanoparticles in contrast to chemisorption observed for functionalized sulfur-containing DAEs and manifested in a bathochromic shift of the absorption maximum of cyclic form [45].

DAE1 also exhibits photochromic properties in solid-phase films obtained by solvent evaporation after deposition of DAE solution in ACN or in DMSO on a quartz plate (fig. 4, *b*). Bathochromic shift of the absorption band of the cyclic form of DAE1 observed in solid-phase layers as compared to solutions is probably due to an ordered arrangement of molecules in solid-phase layers.

From table 3 and in fig. 4, *c, d* it is seen that presence of noble metal nanoparticles in solid-phase films results in insignificant growth of light sensitivity value $\Delta D_B^{phot}/D_A$ (compared to films without nanoparticles). It is probably caused by specific nature of DAE molecules interaction with surface of metal nanoparticles and to contribution of plasmon effects depending on the value of overlapping in metal nanoparticle plasmon excitation band and absorption bands of initial open (A) and photoinduced cyclic (B) forms of DAE1 [26].

Varying the material and size of metal nanoparticles, it is possible to manage parameters of photochromic processes in nanocomposites [46]. In addition, the presence of metal nanoparticles allows their use as contacts in molecular photocontrolled electric signal switches based on photochromic nanocomposites containing DAE [4,23].

For the composite systems „semiconductor nanoparticle–of DAE1 molecule“ (containing QD525 luminescing at wave length $\lambda = 525$ nm, and DAE1) both in solutions and in solid-phase and polymer films, the phenomenon of reversible change in QD fluorescence

Table 4. Absorption and fluorescence characteristics of photochromic nanostructured systems based on DAE1 and QD525 CdSe/ZnS

System	State	λ_A^{max}, nm (D_A)	λ_B^{max}, nm	ΔD_B^{phot}	λ_{QD}^{Fl}, nm	I_0^{Fl}, arb. units	I^{Fl}, arb. units
DAE 1	Solution in toluene	357 (0.64)	519	0.64	–	–	–
DAE 1 + QD525		355 (0.58)	511	0.42	527	156	9
DAE 1	Amorphous film	360 (0.03)	519	0.10	–	–	–
DAE 1 + QD525		359 (0.02)	536	0.009	530	0.092	0.035
DAE 1	Polymer film PMMA	358 (0.21)	520	0.09	–	–	–
DAE 1 + QD525		365 (0.28)	517	0.20	523	74	58
DAE 1	Polymer film AS	–	–	–	–	–	–
DAE 1 + QD525		352 (0.30)	514	0.23	520	41	14

Note. λ_A^{max}, λ_B^{max} — wave lengths of absorption band maxima in initial open and photoinduced cyclic form of DAE, λ_{QD}^{Fl} — wave length of QD fluorescence band maximum; ΔD_B^{phot} — photoinduced variation of optical density in maximum of absorption band of photoinduced cyclic form of DAE in photoequilibrium state; I_0^{Fl}, I^{Fl} — intensities of QD fluorescence bands before and after UV radiation, accordingly.

intensity symbasically to photochromic transformations of DAE1 was found (fig. 5, table 4). This testifies to the possibility of inductive-resonance transfer of excitation energy (FRET) from QD to cyclic DAE form due to the overlapping of the photochromic absorption band and QD fluorescence band and the possibility of implementing nanostructured recording media with non-destructive fluorescence optical information readout.

In addition, by changing the excitation wave length of polymer systems based on QD525 and DAE1, it is possible to perform phototranslation of fluorescence. In this case, quenching of radiation with wave length $\lambda = 525$ nm and simultaneous appearance of fluorescence of cyclic DAE1 form in the spectral region with maximum at 620 nm (fig. 5, *d*, curves *4, 5, 6*) is observed.

The results obtained (table 4) allow us to conclude that the fluorescence intensity modulation in the QD525−DAE1 system takes place both in solutions and in solid-state films. Both fluorescence intensity and fluorescence intensity modulation efficiency (depth) are significantly higher in solution.

Modulation of fluorescence intensity may be due to changes in the quantum yield of QD fluorescence due to the transfer of excitation and/or charge energy to DAE1 molecules located in close proximity, as well as an internal filter effect (i. e., absorption of fluorescence light quanta by DAE1 molecules in closed form B). Using the experimental data obtained, the attenuation of the QD emission intensity due to the internal filter effect was estimated. It was found that the attenuation of emission due to this effect is 47% for the QD525-DAE1 complex (in toluene) with a total reversible photoinduced attenuation of fluorescence emission of this system of 94%. To elucidate the mechanism of fluorescence modulation, the time dependence of QD fluorescence decay time during photoinduced changes of DAE1 was investigated. It turned out that fluorescence decay kinetics of the studied QDs was essentially non-monoexponential. To describe kinetics of QD525, it is necessary to use at least 3 exponential components with lifetime $\tau_1 \sim 2$ ns, $\tau_2 \sim 7$ ns and $\tau_3 \sim 18$ ns (for solutions of QD525-DAE1 complexes); $\tau_1 \sim 0.7$ ns, $\tau_2 \sim 5$ ns and $\tau_3 \sim 16$ ns (for solid-phase amorphous films of QD525-DAE1 complexes on quartz); $\tau_1 \sim 3$ ns, $\tau_2 \sim 9$ ns and $\tau_3 \sim 25$ ns (for solid-phase films of QD525-DAE1 complexes in polymer PMMA). It is assumed that the formation of the QD525-DAE1 complex (due to specific interactions between QD525 and DAE1 molecules in open form A) leads to the appearance of an additional radiation-free deactivation channel and to a certain decrease in the average lifetime of the excited state of QD [30].

The results obtained (table 5) show that the reversible photoisomerization of DAE1 due to UV and visible irradiation significantly affects the QD fluorescence lifetime, which suggests a significant contribution of the FRET mechanism in modulating the QD fluorescence intensity.

In case of polymer films, in contrast to the other three matrices (table 5), reversible modulation (with significant modulation depth) is observed only for the average lifetime $\langle \tau^{\alpha} \rangle$ in amplitude (but not for $\langle \tau \rangle$). This may be due to the fact that the heterogeneity of the emitting centers in the PMMA film may increase due to interactions of the polymer molecules with the QD-DAE1 systems. Then, it is more correct to estimate the kinetics of QD luminescence decay not by the average lifetime $\langle \tau \rangle$ by contribution,

$$\langle \tau \rangle = \frac{\sum_i \alpha_i \tau_i^2}{\alpha_i \tau_i}, \quad (1)$$

but by average lifetime $\langle \tau^{\alpha} \rangle$ by amplitude

$$\langle \tau^{\alpha} \rangle = \frac{\sum_i \alpha_i \tau_i}{\alpha_i}, \quad (2)$$

where α_i, τ_i — pre-exponential multiplier and lifetime of i-th component, accordingly.

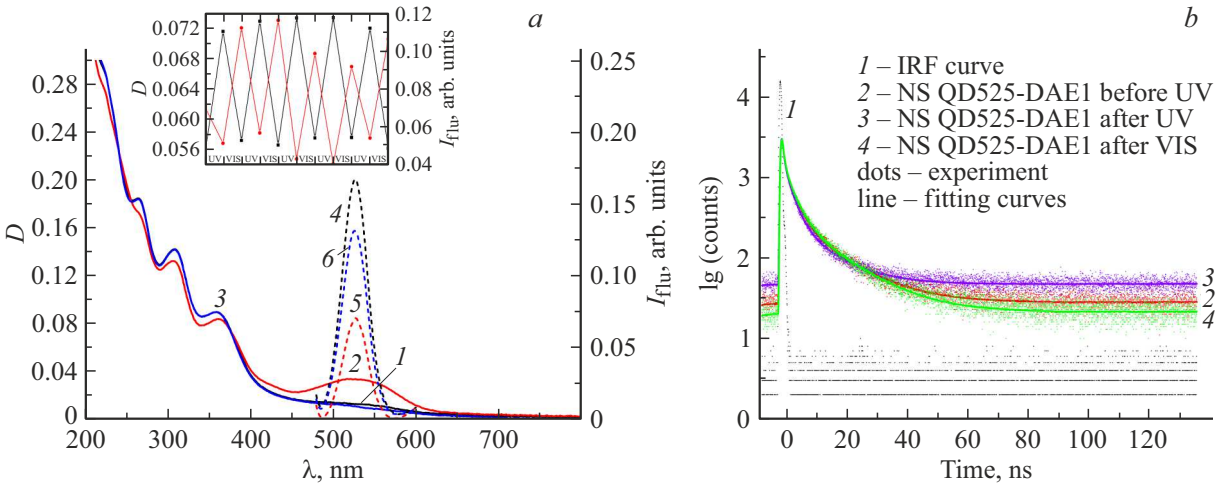

Figure 6. (*a*) Absorption spectra (curves *1–3*) and fluorescence spectra at excitation wave length 500 nm (*4–6*) of polymer nanospheres containing QD525 and DAE1, in water before (*1, 4*), after UV radiation (*2, 5*) and visible (*3, 6*) light exposure. The insert demonstrates variation of optical density (black curves) on wave length 532 nm and intensity of fluorescence (red) on wave length 525 nm of polymer nanospheres containing QD525 and DAE1, after serial UV radiation ($\lambda = 365$ nm, $t = 150$ s) and visible ($\lambda = 514$ nm, $t = 150$ s) light exposure. (*b*) Curves of fluorescence decay of aqueous solutions of nanospheres containing DAE1 before (*b, 2*), after UV radiation (*b, 3*) and after visible (*b, 4*) radiation.

Table 5. Average lifetime $\langle\tau\rangle$ by contribution and average lifetime $\langle\tau^{\alpha}\rangle$ by amplitude of QD525 fluorescence in process of photochromic transformations of DAE1 in various systems

System (state)	$\langle\tau_0\rangle$, ns	$\langle\tau_{UV}\rangle$, ns	$\langle\tau_{VIS}\rangle$, ns	$\langle\tau_0^{\alpha}\rangle$, ns	$\langle\tau_{UV}^{\alpha}\rangle$, ns	$\langle\tau_{VIS}^{\alpha}\rangle$, ns
Solution in toluene	12.93	11.99	12.84	9.29	7.73	9.29
Solid-phase amorphous film	9.66	7.38	10.00	4.00	2.47	4.35
Polymer PMMA film	11.84	11.96	11.96	8.10	6.63	8.80
Polymer nanospheres	7.05	5.39*	7.42**	2.08	1.66*	2.11**

Note. $\langle\tau_0\rangle(\langle\tau_0^{\alpha}\rangle)$, $\langle\tau_{UV}\rangle(\langle\tau_{UV}^{\alpha}\rangle)$, $\langle\tau_{VIS}\rangle(\langle\tau_{VIS}^{\alpha}\rangle)$ — lifetimes of QD525 before, after UV radiation for 15 s and after visible light exposure ($\lambda = 514$ nm) for 30 s accordingly. For polymer nanospheres time of UV radiation 20 s* and visible light exposure is 45 s**.

Similar spectral-kinetic studies were also performed for synthesized polymeric nanospheres containing QD525 and DAE1 molecules. Photoinduced isomerization of DAE1 molecules affects the fluorescence parameters of QD525 in nanospheres (fig. 6, table 5). The estimated decrease in the luminescence intensity of nanospheres due to changes in the quantum yield of QD fluorescence is ~ 53%. Influence of the internal filter effect does not exceed 3%, which indicates the efficiency of the developed photochromic nanospheres compared to the previously described nanostructured systems [30,31]. To elucidate the mechanism of QD fluorescence quenching by DAE1 molecules in nanospheres, the kinetics of QD fluorescence decay during photoinduced change of DAE1 was investigated (fig. 6, *b*, table 5).

It was found that the decay curve is satisfactorily approximated by three exponents with lifetime $\tau_1 \sim 0.5$ ns, $\tau_2 \sim 3$ ns and $\tau_3 \sim 14$ ns. The observed changes in QD fluorescence intensity due to phototransformations of DAE1 molecules are also repeated in the reversible changes in their fluorescence duration values. The $\langle\tau\rangle$ fluorescence duration reduction of nanospheres after UV irradiation is restored completely after visible light exposure. Therefore, it can be argued that FRET is the mechanism that determines the modulation of QD fluorescence intensity in synthesized nanospheres during reversible photoisomerization of DAE1 molecules implanted in them.

FRET modeling

In order to estimate the parameters of the „QD525-DAE1“nanostructured system that are optimal for the FRET process, a computer simulation of this system was performed.

Based on spectral data for complexes of QD525 with DAE1 molecules according to known models [30,31], the value of the critical Ferster radius $R_{01} = 5.60$ nm (with values of donor-acceptor dipole pair orientation coefficient $\kappa^2 = 0.67$, refractive index $n_{ref} = 1.4969$, QD fluorescence quantum yield $\Phi = 0.628$).

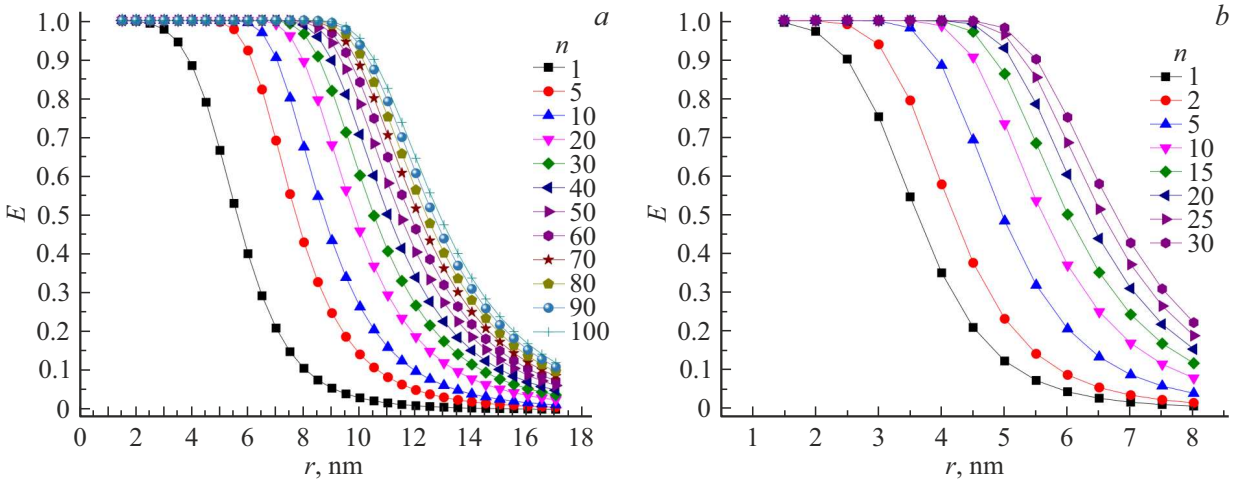

Figure 7. Dependence of QD-DAE1 fluorescence modulation efficiency (in solution (a) and in polymeric nanospheres (b)) on the distance r between QD and DAE1 and on the number n of DAE1 molecules on QDs (at 30% of colored DAE1 form molecules).

For polymeric nanospheres based on molar absorption coefficient values (for DAE1 in toluene with $\lambda = 370$ nm $\varepsilon = 1.33 \cdot 10^4\,\mathrm{M^{-1}cm^{-1}}$ and for CdSe QD of diameter 2.7 nm $\varepsilon = 5 \cdot 10^4\,\mathrm{M^{-1}cm^{-1}}$ [47]), the average number of DAE1 molecules per QD in a nanosphere is calculated: $n \sim 4{-}8$. According to the estimate, the fraction of photoinduced B form of DAE1 molecules in the state of equilibrium of A and B forms is about 30%. With the values of donor-acceptor dipole pair orientation coefficient $\kappa^2 = 0.48$, refractive index $n_{\mathrm{ref}} = 1.50$, QD fluorescence quantum yield $\Phi = 0.0628$, the critical Ferster radius for polymeric nanospheres is $R_{02} = 3.60$ nm.

By means of simulations, the FRET efficiency was evaluated at different ratios of the number of DAE1 molecules per QD. The FRET efficiency for donor D (QD) surrounded by n acceptor A (DAE1) molecules as measured by fluorescence duration [31]

$$E(\tau) = 1 - \frac{\tau_{\mathrm{DA}n}}{\tau_{\mathrm{D}}}, \qquad (3)$$

$\tau_{\mathrm{DA}n}$ — the lifetime of the excited state of the donor in the presence of the acceptor,

$$\frac{1}{\tau_{\mathrm{DA}n}} = \frac{1}{\tau_{\mathrm{D}}} \prod_{i=1}^{n} \left(1 + \left(\frac{R_0}{r_i}\right)^6\right), \qquad (4)$$

τ_{D} —the lifetime of the excited state of the donor in the absence of the acceptor, R_0 — Ferster radius, r_i —the distance between the i-th molecule of the acceptor and the donor.

The results of calculating the dependencies of QD-DAE1 fluorescence modulation efficiency on the distance r between QD and DAE1, on the number n of DAE1 molecules on QD, on the quantum yield of QD fluorescence ($\Phi = 0.6$ for solution, $\Phi = 0.06$ for polymeric nanospheres) and on the percentage of molecules of the colored form of DAE1 are shown in fig. 7.

At a fixed value of R_0, the efficiency of quenching of QD fluorescence due to energy transfer to colored DAE1 photoisomers depends on the distance between the donor (QD525) and acceptor (DAE1 molecule) energy, as well as on the number of acceptors in the environment of one donor.

Fig. 7 shows that high values ($\sim$ 0.8) of the donor fluorescence quenching factor are achieved at distances r between donors and acceptors within 6.5 nm, if there are at least 5 DAE1 molecules per one QD with a fluorescence quantum yield in the complex of 60% (in solution), or at $r = 4$ nm, if there are at least 5 DAE1 molecules per one QD with a fluorescence quantum yield of 6% (in polymeric nanospheres).

From the analysis of the results obtained (fig. 7, b) we can estimate the value of the distance $r \sim 4$ nm between QD and DAE1 at the following parameter values: 30% molecules of colored form DAE1, QP fluorescence quantum yield $\Phi = 0.06$, Ferster radius $R_{02} = 3.60$ nm, average number of DAE1 molecules per QD in the nanosphere approximately $n \sim 6$ and depth (efficiency) of fluorescence intensity modulation of nanospheres ~ 0.57.

Photoinduced changes of vibrational spectra of photochromic systems based on DAE1

Photoinduced reversible changes in the structure of photochromic molecules in various matrices can also manifest themselves (along with electronic absorption spectra) in vibrational spectra.

Experimental spectra of IR absorption and RS light of DAE1 in powder, as well as SERS light spectra of the studied nanocomposite systems based on this DAE (and IR absorption spectra of DAE1 solid-phase films) and their photoinduced changes in the process of photochromic transformations of molecules are shown in fig. 8.

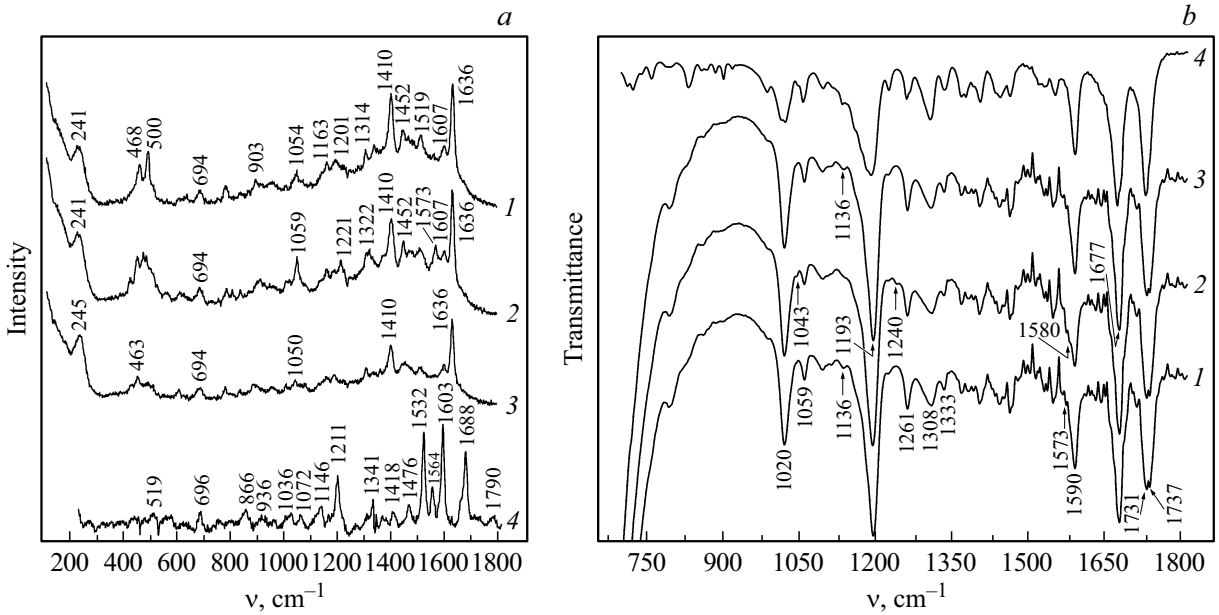

Figure 8. Raman spectra of light (*a*, curve *4*) and IR absorption (*b*, *4*) of DAE1 powder. SERS light spectra (*a, 1–3*) [28] of solid-phase composite nanostructures „metal nanoparticle–photochrome“ (based in compound of DAE1 and silve sol on quartz substrate) at $\lambda_{ex} = 633$ nm: before radiation (*a, 1*), after UV radiation (*a*, 2), after subsequent laser radiation with wave length $\lambda = 633$ nm (*a, 3*). Solid-phase composite nanostructures are obtained from solutions in methanol. IR absorption spectra (*b, 1–3*) of DAE1 film from toluene solution: before radiation (*b, 1*), after UV radiation (*b, 2*), after subsequent exposure to visible light (*b, 3*).

By quantum-chemical methods (using computational methods and bases optimized for the given problems) we obtained refined data on the structure and vibrational spectra of photochromic DAE1 molecule in open A and cyclic B forms (fig. 9). Using this data the interpretation of experimental vibrational spectra (IR, RS and SERS) was carried out. In calculated spectra the bands caused by planar vibrations of bound cycles are the most intense. For a cyclic form having a planar configuration, there is π-coupling between cycles. As a result of photoinduced reaction of cycloreversion, C9-C19 bond breaks, causing the planes of cycles III, IV and cycles V, VI of DAE1 molecule to rotate relative to each other at an angle of about 70°. In this case, the intensity of RS bands decreases by an order of magnitude.

The highest intensity in experimental spectra of both IR absorption and RS (SERS) of DAE1 is observed for bands related to flat valent and deformation oscillations (around 500, 1200, 1410, 1607, 1636 cm^{-1} — SERS and around 1020, 1193, 1590, 1677, 1733 cm^{-1} — IR spectra). Bands around 1200, 1600, 1680 cm^{-1} are intense in spectra of IR absorption and RS (SERS) of light. This can be explained by the proximity of the probabilities of vibrational transitions due to the specific local symmetry of molecules [28]. The greatest intensification is experienced by the RS bands around 500, 1410, 1636 cm^{-1}, the main contribution to which is made by planar vibrations, which is manifested in the SERS spectra of solid-phase composite nanostructures „metal nanoparticle–photochrome“ (fig. 8, *a*, curves *1–3*). Smooth spheroidal shape of silver nanoparticles (without small grains with sharp surface fractures), as well as their size suggest that the greatest contribution to the amplification of the RS signal of DAE1 molecules adsorbed on these particles, is made by plasmon mechanisms, rather than other electromagnetic amplification mechanisms, such as those associated with a giant increase in electromagnetic fields and their gradients on the surface fractures with small radii of curvature [48].

Phototransformations of composite nanostructures „metal nanoparticle–photochrome“ are manifested by changes in the relative intensity of bands in the vibrational spectra of the DAE1 compound related to vibrations of the bond involved in the photoisomerization reaction [28]. Successive irradiation of the sample first with UV and then with visible light leads first to an increase in the relative intensity of the bands around 1221 and 1573 cm^{-1} (fig. 8, *a* (Fig. 8, *a*, curve *2*) and then to a return of the SERS spectrum shape to the original (fig. 8, *a*, curves *1, 3*). These spectral changes show the photochromic properties of this nanocomposite. Reversible changes in the relative intensities of bands related to $C_9–C_{19}$ bond vibrations are also observed in the IR absorption spectrum (bands around 1043, 1240, 1580 cm^{-1}).

Important evidence of chemical interaction between DAE1 molecule and metal surface is the presence of a band of about 240 cm^{-1} (due to the vibration of the molecule-metal bond [49]) in the SERS spectra of nanocomposites based on DAE1 compound obtained from a solution in methanol (fig. 8, *a*, curves *1–3*), in contrast to similar nanocomposites obtained from solution in acetonitrile [28].

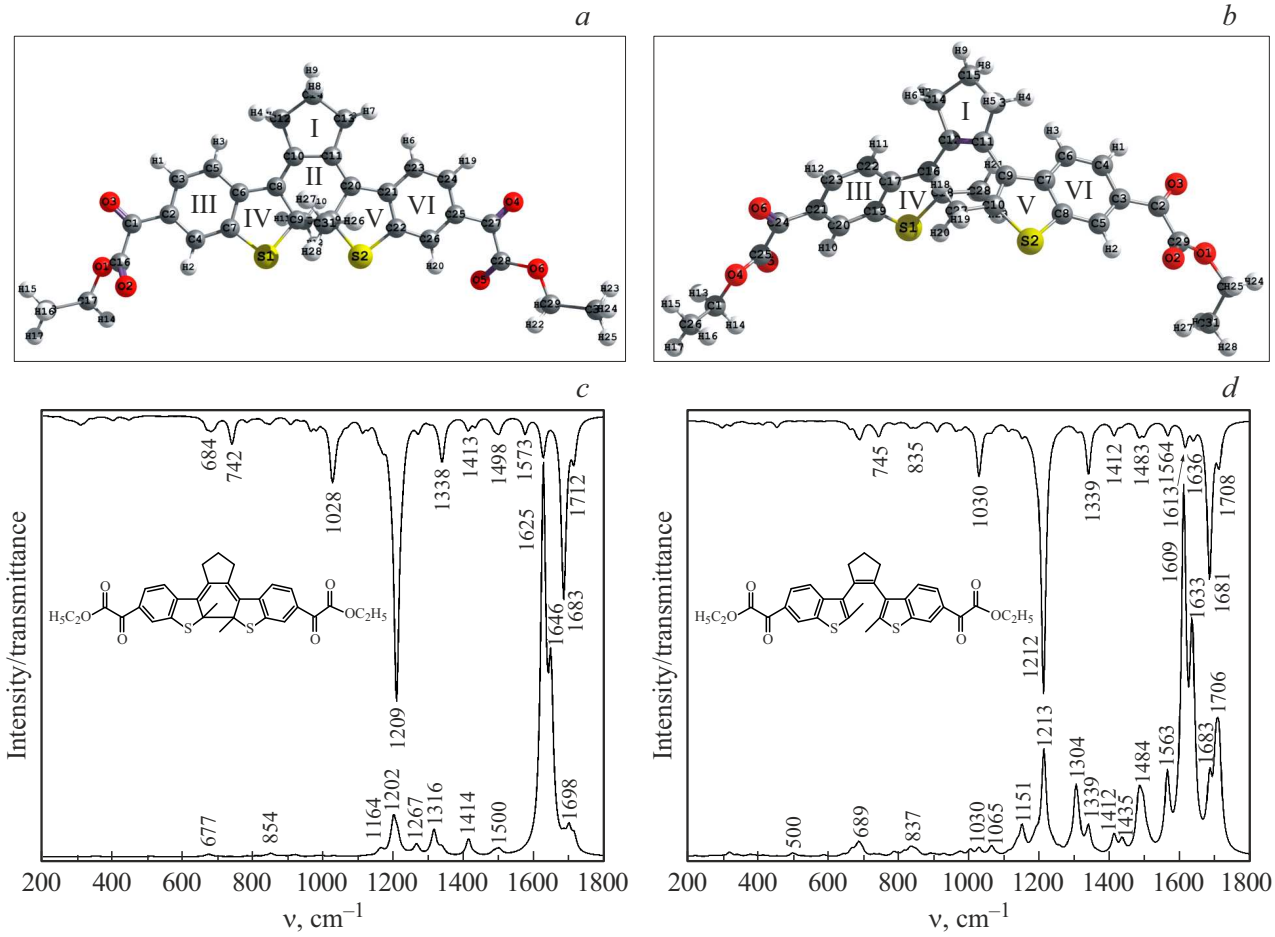

Figure 9. Optimized geometry of cyclic (*a*) and open (*b*) forms of DAE1 molecule. Calculated dependences of IR absorption intensity (upper graphs) and RS activity (lower graphs) on the frequency of cyclic (*c*) and open (*d*) forms of DAE1 molecule.

Conclusion

Spectral properties of generated composite nanostructures „nanoparticle–photochromic molecule“ consisting of nanoparticles Ag, Au (or QD) with a shell of photochromic DAE molecules were studied. It was found that these nanocomposites both in solutions and in solid-phase layers possess photochromic properties (which manifest themselves in reversible photoinduced changes in the electronic and vibrational spectra of DAE) similar to the photochromic transformations of DAE in solutions and in solid-phase layers containing no nanoparticles.

Quantum-chemical study of electronic and vibrational spectra and obtaining cross sections of DAE1 potential energy surfaces allowed the numerical parameters of structure, energy, and electronic properties to be estimated during photoisomerization of the DAE1 molecule.

Photoinduced change in the structure of „metal nanoparticle–photochrome“ nanocomposites manifests itself in changes in the relative intensities of bands in the SERS and IR spectra, primarily the bands due to valent vibrations of the C_9-C_{19} bond, involved in the reversible photoisomerization reaction of DAE.

Based on the results of modeling the process of inductive-resonance excitation energy transfer between CdSe/ZnS QD and photochromic molecules, photo-controlled fluorescence systems QD525-DAE1 were created. QD525-DAE1 systems both in solutions and in solid-state layers, as well as in polymeric nanospheres exhibit modulation of QD fluorescence intensity and duration due to reversible photoisomerization of the photochromic compound molecules. Observed modulation of fluorescence intensity in these systems is due to both inductive resonance energy transfer from QD to photoinduced cyclic form of DAE molecules (FRET) (estimated by $\sim 47\%$ for solutions of QD525-DAE1 complexes, $\sim 53\%$ for polymeric nanospheres) and the effect of fluorescence overabsorption by photochromic molecules (estimated by $\sim 47\%$ for QD525-DAE1 complex solutions, $\sim 3\%$ for polymeric nanospheres), which is much better than our earlier results for other DAE [30,31].

Critical Ferster radii for the QD525-DAE1 pair ($R_{01} = 5.60$ nm in solutions and $R_{02} = 3.60$ nm in poly-

meric nanospheres) and FRET efficiency at different ratios of number of DAE1 molecules per QD were determined by simulation.

Composite nanostructured elements based on photochromic DAE1 that reversibly change their absorption and fluorescence properties under the action of light according to the photochromic transformations of DAE were obtained, which can be used in the development of optoelectronic photocontrolled molecular switches as well as bio- and chemosensors.

Acknowledgments

The authors express their sincere gratitude to V.I. Stepuro and A.G. Starikov for their participation in the discussion of the results presented in this work.

Funding

This paper was financially supported by the Belarusian Republican Foundation for Fundamental Research (grant № F21RM-134), the Ministry of Education of the Republic of Belarus (assignment 1.5 GPNI „Photonics and Electronics for Innovation“) and the Ministry of Science and Higher Education of the Russian Federation within the framework of the state assignment of the RAS Research Center „Crystalography and Photonics“ for the analysis of the spectral properties of photochromic systems.

Conflict of interest

The authors declare that they have no conflict of interest.

References

[1] C. Joachim, J.K. Gimzewski, A.A. Aviram. Nature, **408**, 541 (2000). DOI:10.1038/35046000
[2] R.L. Carroil, C.B. Gorman. Angew. Chem. Int. Ed., **41**, 4378 (2002). DOI: 10.1002/1521-3773(20021202)41:23¡4378::AID-ANIE4378¿3.0.CO;2-A
[3] M. Irie. Molecular switches, ed. by B.L. Feringa (Wiley-VCH, Weinheim, 2001), ch. 5, p. 37–60.
[4] M. Irie, T. Fukaminato, K. Matsuda, S. Kobatake. Chem.Rev., **114**, 12174 (2014). DOI: 10.1021/cr500249p
[5] H. Tian, S. Yang. Chem. Soc. Rev., **33**, 85 (2004). DOI: 10.1039/B302356G
[6] Molecular switches, ed. by B.L. Feringa (Wiley-VCH, Weinheim, 2001).
[7] V.A. Barachevsky. Org. Photon. Photovolt., **3** (1), 8 (2015). DOI: 10.1515/oph-2015-0003
[8] H. Yamaguchi, M. Ikeda, K. Matsuda, M. Irie. Bull. Chem. Soc. Jpn., **79**, 1413 (2006). DOI: 10.1246/bcsj.79.1413
[9] T. Kubernac, S.J. Molen, B.J. Wees, B.L. Feringa. Chem. Commun., 3597 (2006). DOI: 10.1039/B609119A
[10] N. Katsonis, T. Kubernac, M. Walko. Adv. Mater., **18**, 1397 (2006). DOI: 10.1002/adma.200600210
[11] S. Perrier, F. Maurel, J. Aubard. J. Phys. Chem. A., **111**, 9688 (2007). DOI: 10.1021/jp073436a
[12] B.L. Feringa. J. Org. Chem., **72**, 6635 (2007). DOI: 10.1021/jo070394d
[13] K. Matsuda, H. Yamaguchi, T. Sakano, M. Ikeda, N. Tanifuji, M. Irie. J. Phys. Chem. C., **112**, 17005 (2008). DOI:10.1021/jp807479g
[14] H. Nishi, T. Asahi, S. Kobatake. J. Phys. Chem. C, **113**, 17359 (2009). DOI: 10.1021/jp906371k
[15] H. Yamaguchi, K. Matsuda, M. Irie. J. Phys. Chem. C, **111**, 3853 (2007). DOI:10.1021/jp065856q
[16] M. Ikeda, N. Tanifuji, H. Yamaguchi, M. Irie, K. Matsuda. Chem. Commun., **13**, 1355 (2007). DOI: 10.1039/B617246F
[17] M.-S. Wang, G. Xu, Z.-J. Zhang, G.-C. Guo. Chem. Commun., **46**, 361 (2010). DOI:10.1039/B917890B
[18] A. Nitzan, L.E. Brus. J. Chem. Phys., **74**, 5321 (1981). DOI: 10.1063/1.441699
[19] A. Nitzan, L.E. Brus. J. Chem. Phys., **75**, 2205 (1981). DOI: 10.1063/1.442333
[20] K. Watanabe, D. Menzel, N. Nilius, H.-J. Freund. Chem. Rev., **106** (10), 4301 (2006). DOI: 10.1021/cr050167g
[21] K. Ueno, H. Misawa. J. Photochem. Photobiol. C, **15**, 31 (2013). DOI: 10.1016/j.jphotochemrev.2013.04.001
[22] G.T. Vasilyuk, S.A. Maskevich, A.E. German, I.F. Sveklo, B.S. Luk'yanov, L.A. Ageev. High Ener. Chem., **43** (7), 521 (2009). DOI: 10.1134/$S_0$018143909070017
[23] R. Klajn, J.F. Stoddart, B.A. Grzybowski. Chem. Soc. Rev., **39**, 2203 (2010). DOI: 10.1039/B920377J
[24] J. Zhang, Q. Zou, H. Tian. Adv. Mater., **25**, 378 (2013). DOI:10.1002/adma.201201521
[25] J. Cusido, E. Deniz, F.M. Raymo. Eur. J. Org. Chem., (13), 2031 (2009). DOI: 10.1002/ejoc.200801244
[26] G.T. Vasilyuk, V.F. Askirka, A.E. German, I.F. Sveklo, V.M. Yasinsky, A.A. Yaroshevich, O.I. Kobeleva, T.M. Valova, A.O. Ayt, V.A. Barachevsky, V.N. Yarovenko, M.M. Krayushkin, S.A. Maskevich. Zh. prikl. spektrosk., 84 (4), 570 (2017) (in Russian). [J. Appl. Spectrosc., **84** (4), 588 (2017)]. DOI: 10.1007/s10812-017-0515-2
[27] D.S. Filimonenko, V.M. Yasinskii, G.T. Vasilyuk, S.A. Maskevich, A.E. German, V.F. Oskirko, B.S. Lukyanov, V.I. Minkin. In: Proc. Int. Conf. NANOMEETING-2015 (Minsk, 2015), p. 80.
[28] G.T. Vasilyuk, S.A. Maskevich, V.F. Askirka, A.V. Lavysh, S.A. Kurguzenkov, A.E. German, I.F. Sveklo, V.M. Yasinsky, A.A. Yaroshevich, O.I. Kobeleva, T.M. Valova, A.O. Ayt, V.A. Barachevsky, V.N. Yarovenko, M.M. Krayushkin. Zh. prikl. spektrosk., **84** (5), 710 (2017) (in Russian). [J. Appl. Spectrosc., **84** (4), 700 (2017)]. DOI: 10.1007/s10812-017-0543-y
[29] V.A. Barachevsky, O.V. Venidiktova, O.I. Kobeleva, A.M. Gorelik, A.O. Ayt, M.M. Krayushkin, A.R. Tameev, G.I. Sigeikin, M.A. Saveliev, G.T. Vasiluyk. IEEENANO - 2015: Nanotechnology, Proc. IEEE, 358 (2015).
[30] P.V. Karpach, A.A. Scherbovich, G.T. Vasilyuk, V.I. Stsiapura, A.O. Ayt, V.A. Barachevsky, A.R. Tuktarov, A.A. Khuzin, S.A. Maskevich. J. Fluoresc., **29** (6), 1311 (2019). DOI: 10.1007/s10895-019-02455-4
[31] A.A. Scherbovich, S.A. Maskevich, P.V. Karpach, G.T. Vasilyuk, V.I. Stsiapura, O.V. Venidiktova, A.O. Ayt, V.A. Barachevsky, A.A. Khuzin, A.R. Tuktarov, M. Artemyev. J. Phys. Chem. C, **124**, 27064 (2020). DOI: 10.1021/acs.jpcc.0c06651

[32] V.A. Barachevsky, O.I. Kobeleva, A.O. Ayt, A.M. Gorelik, T.M. Valova, M.M. Krayushkin, V.N. Yarovenko, K.S. Levchenko, V.V. Kiyko, G.T. Vasilyuk. Opt. Mater., **35**, 1805 (2013). DOI: 10.1016/j.optmat.2013.03.005
[33] V.A. Barachevsky, O.I. Kobeleva, O.V. Venidiktova, A.O. Ayt, G.T. Vasilyuk, S.A. Maskevich, M.M. Krayushkin. Kristallografiya **64** (4), 820 (in Russian) (2019). [Crystallogr. Rep., **64** (5), 823(2019)]. DOI: 10.1134/S1063774519050055
[34] V.A. Barachevsky, O.V. Venidiktova, T.M. Valova, A.M. Gorelik, R. Vasiliev, A. Khuzin, A.R. Tuktarov, P.V. Karpach, V.I. Stsiapura, G.T. Vasilyuk, S.A. Maskevich. Photochem. Photobiol. Sci., **18**, 2661 (2019). DOI: 10.1039/C9PP00341J
[35] P.C. Lee, D. Meisel. J. Phys. Chem., **86**, 3391(1982). DOI: 10.1021/j100214a025
[36] C.N. Lok, C.-M. Ho, R. Chen, Q.-Y. He, W.-Y. Wing-Yiu Yu, H. Sun, P.K.-H. Paul Kwong-Hang Tam, J.-F. Jen-Fu Chiu, C.-M. Chi-Ming Che. J. Biol. Inorg. Chem., **12**, 527(2007). DOI: 10.1007/s00775-007-0208-z
[37] J. Turkevich. Gold Bull., **18** (3), 8 (1985). DOI:10.1007/BF03216574
[38] J. Kimling, M. Maier, B. Okenve, V. Kotaidis, H. Ballot, A. Plech. JPC B, **110**, 15700 (2006). DOI:10.1021/jp061667w
[39] A. Fedosyuk, A. Radchanka, A. Antanovich, A. Prudnikau, M.A. Kvach, V. Shmanai, M. Artemyev. Langmuir, **32** (8), 1955 (2016). DOI: 10.1021/acs.langmuir.5b04602
[40] A.A. Maskevich, V.I. Stepuro, S.A. Kurguzenkov, A.V. Lavysh. Vestnik Grodn. Gos. Universiteta, **3** (159), 107 (2013) (in Russian).
[41] D.V. O'Connor, D. Phillips. Time-correlated Single Photon Counting, (Acad. Press, N.Y., 1984).
[42] A.D. Becke. J. Chem. Phys., **98** (3), 5648 (1993). DOI: 10.1063/1.464913
[43] A.D. Becke. Phys. Rev. A, **38** (6), 3098 (1988). DOI: 10.1103/PhysRevA.38.3098
[44] C. Lee, W. Yang, R.G. Parr. Phys. Rev., **37** (2), 785 (1988). DOI: 10.1103/PhysRevB.37.785
[45] O.I. Kobeleva, T.M. Valova, V.A. Barachevsky, M.M. Krayushkin, B.V. Lichitsky, A.A. Dudinov, O.Yu. Kuznetsova, G.E. Adamov, E.P. Grebennikov. Opt. spektrosk. (in Russian), **109** (1), 106 (2010) [Opt. Spectr., **109** (1), 101 (2010)]. DOI: 10.1134/$S_0$030400X10070167
[46] G.T. Vasilyuk. Vestnik fonda fundamentalnykh issledovaniy, (2), 102 (2021) (in Russian).
[47] W.W. Yu, L. Qu, W. Guo, X. Peng. Chem. Mater., **15** (14), 2854 (2003). DOI: 10.1021/cm034081k
[48] A.M. Polubotko, V.P. Chelibanov. Opt. Spectr., **120** (1), 86 (2016) (in Russian). DOI: 10.1134/$S_0$030400X1512019X
[49] I.R. Nabiev, R.G. Efremov. Spektroskopiya gigantskogo kombinatsionnogo rasseyaniya i ee primenenie k izucheniyu biologicheskikh molekul (VINITI, M.,1989) (in Russian).